Analytical Methods

International Edition: DOI: 10.1002/anie.201802937
German Edition: DOI: 10.1002/ange.201802937

Mass Spectrometry Imaging with Isomeric Resolution Enabled by Ozone-Induced Dissociation

*Martin R. L. Paine, Berwyck L. J. Poad, Gert B. Eijkel, David L. Marshall, Stephen J. Blanksby, Ron M. A. Heeren, and Shane R. Ellis**

Abstract: *Mass spectrometry imaging (MSI) enables the spatial distributions of molecules possessing different mass-to-charge ratios to be mapped within complex environments revealing regional changes at the molecular level. Even at high mass resolving power, however, these images often reflect the summed distribution of multiple isomeric molecules, each potentially possessing a unique distribution coinciding with distinct biological function(s) and metabolic origin. Herein, this chemical ambiguity is addressed through an innovative combination of ozone-induced dissociation reactions with MSI, enabling the differential imaging of isomeric lipid molecules directly from biological tissues. For the first time, we demonstrate both double bond- and sn-positional isomeric lipids exhibit distinct spatial locations within tissue. This MSI approach enables researchers to unravel local lipid molecular complexity based on both exact elemental composition and isomeric structure directly from tissues.*

Mass spectrometry imaging (MSI) is a powerful method for studying the spatial distributions of molecules throughout heterogeneous surfaces (for example, biological tissues) and their association with disease-driven chemical alterations.[1] More broadly, MSI has enabled untargeted and spatially resolved chemical analysis to unravel complex biomolecular processes.

In biological applications, MSI technologies including matrix-assisted laser desorption ionization (MALDI) and desorption electrospray ionization give access to information on a broad range of analytes across an array of substrates.[2] In most applications, MSI generates distributions of a selected mass-to-charge (m/z) ratio with routine spatial resolutions of 10–100 μm. These data, especially when acquired with high mass-resolving power, are often interpreted as molecular distributions. While such representations have their own value (for example, tissue differentiation and classification), their correlation with biochemical composition and metabolic activity is tenuous, as these signals represent the composite distributions of a range of isomers. Tandem mass spectrometry (MS/MS) can aid in certain cases[3] but fails for structural isomers that yield identical product ions under conventional ion activation conditions. Methods enabling isomeric resolution are required to reach the goal of performing MSI on structurally defined chemical species.

The need for isomer-resolved MSI is most apparent in lipid biology in which the cumulative variation results in more than 100 000 possible lipid structures in the cellular lipidome.[4] In part, this complexity arises because of the presence of structural isomers varying only in fatty acyl chain composition, sites of unsaturation (double bond-positional (db) isomers), and esterification position of fatty acyl chains in glycerolipids (*sn*-positional isomers). While the structural differences between these isomeric variants are subtle, they demarcate distinct biosynthetic origins and biological functions. Isomeric resolution is therefore essential to understand the origin of de novo synthesized lipids from enzymatic processes, such as the action of specific elongase and desaturase enzymes in creating db-isomers.[5] Resolving structural isomers is also vital for a better understanding of disease progression. For instance, the dysregulation of pathways involving the phospholipase A2 (PLA2) family of enzymes, responsible for selective hydrolysis of fatty acids localized to the *sn*-2 position on the glycerol backbone, has been implicated in a variety of cancers.[6] Conventional tandem mass spectrometry (that is, low-energy collision-induced dissociation, CID) provides distinct spectra for different fatty acyl chain combinations, but is largely blind to the presence of regioisomers arising from db- or *sn*-positional variation. By necessity, alternative ion activation strategies have been developed to resolve signals arising from isomeric lipids. These include photochemically activated Paternò–Büchi reactions,[7] ultraviolet photodissociation,[8] electron-based activation,[9] and ozone-induced dissociation (OzID).[10] OzID has proven to be particularly versatile owing to the production of easy to interpret spectra and ability to resolve both db- and *sn*-positional isomers.[10b] Ion mobility coupled with mass spectrometry is another method to resolve isomeric lipids.[11] Application of ion mobility spectrometry to complex biological extracts however, does not always yield mobility separation of isomers and, in instances in which the presence of multiple isomeric contributors is demonstrated,

[*] Dr. M. R. L. Paine, G. B. Eijkel, Prof. Dr. R. M. A. Heeren, Dr. S. R. Ellis
M4I, The Maastricht Multimodal Molecular Imaging Institute,
Division of Imaging Mass Spectrometry, Maastricht University
Postbus 616, 6200 MD Maastricht (The Netherlands)
E-mail: s.ellis@maastrichtuniversity.nl
Dr. B. L. J. Poad, Dr. D. L. Marshall, Prof. S. J. Blanksby
Central Analytical Research Facility, Institute for Future Environments, Queensland University of Technology
2 George St, Brisbane, QLD 4000 (Australia)
Supporting information and the ORCID identification number(s) for the author(s) of this article can be found under: https://doi.org/10.1002/anie.201802937.

the structural differences between them remain to be elucidated. Remarkably, a mixture of isomeric lipids is observed in almost every case in which isomeric resolution is achieved for biological extracts. For example, using photochemical Paternò–Büchi reactions, levels of lipids with double bonds located at the $n-7$ position (with respect to the methyl terminus) were observed to be elevated relative to those of the corresponding $n-9$ isomers in cancerous breast tissue.[12] The relative abundance of db- and *sn*-positional isomers has also been observed to vary dramatically across different tissue types,[12,13] providing a strong motivation to visualize selective and conserved alterations in lipid isomer populations by MSI.

Herein, we present the first report of MSI providing unambiguous isomeric resolution when applied to multiple families of lipid isomers. This was accomplished by the unique coupling of MALDI-MSI with OzID in a linear ion-trap mass spectrometer, which enabled us to visualize highly specific enrichment of multiple isomeric lipids in distinct spatial regions in the rat brain.

OzID spectra were obtained at each pixel of a MALDI-MSI experiment to reveal spatial distributions of distinct lipid isomers in tissues on a modified MALDI-LTQ-Orbitrap Elite mass spectrometer (Figure S1, Supporting Information). Ozonolysis reaction schemes are provided in Supporting Information (Schemes S1 and S2). Prior to analysis tissues were coated with norharmane matrix and sodium acetate to preferentially drive formation of $[M+Na]^+$ ions beneficial for OzID. First, we investigated the distributions of db-isomers corresponding to two abundant mono-unsaturated lipids in rat brain, phosphatidylcholines PC(34:1) and PC(36:1) with acyl chains comprising 34 and 36 carbons, and having relative abundances of circa 100 % and 30 %, respectively, in the full-scan FTMS spectrum. The MALDI-OzID spectrum of $[PC(34:1)+Na]^+$ (Figure 1 a) revealed two sets of product ions consistent with ozonolysis of distinct db-isomers with unsaturation at the $n-9$ (m/z 672.4 and 688.3) and $n-7$ (m/z 700.4 and 716.4) positions. In all cases the assignment of product ions was supported by high mass accuracy measurements obtained using the Orbitrap mass analyzer (Table S1, Supporting Information) and were consistent with the predicted OzID transitions (Scheme S1). We note that owing to the required 10 s reaction time, only a small area of the sample could practically be measured. The on-tissue distribution of the $[PC(34:1)+Na]^+$ precursor ion from the Orbitrap MSI data represents the maximum level of structural detail achievable with current high-mass resolution MSI (Figure 1 b). Yet this only provides the summed distribution of all contributing isomers and reveals a relatively homogenous distribution of $[PC(34:1)+Na]^+$ signal throughout the rat brain, with only a minor elevation of signal observed in the white matter. Activating isomeric resolution through OzID on an adjacent tissue section enabled the distribution of distinct db-isomer populations to be observed. Figure 1 c shows the fractional distribution image (FDI), representing the intensity of $n-7$-related ions as a fraction of all $n-9$ and $n-7$-related ion signals (that is, a higher intensity corresponds to a larger population of the $n-7$ isomer relative to the $n-9$ isomer), revealed enrichment of the $n-7$ isomer in the gray matter. Conversely, enrichment in signals characteristic of the

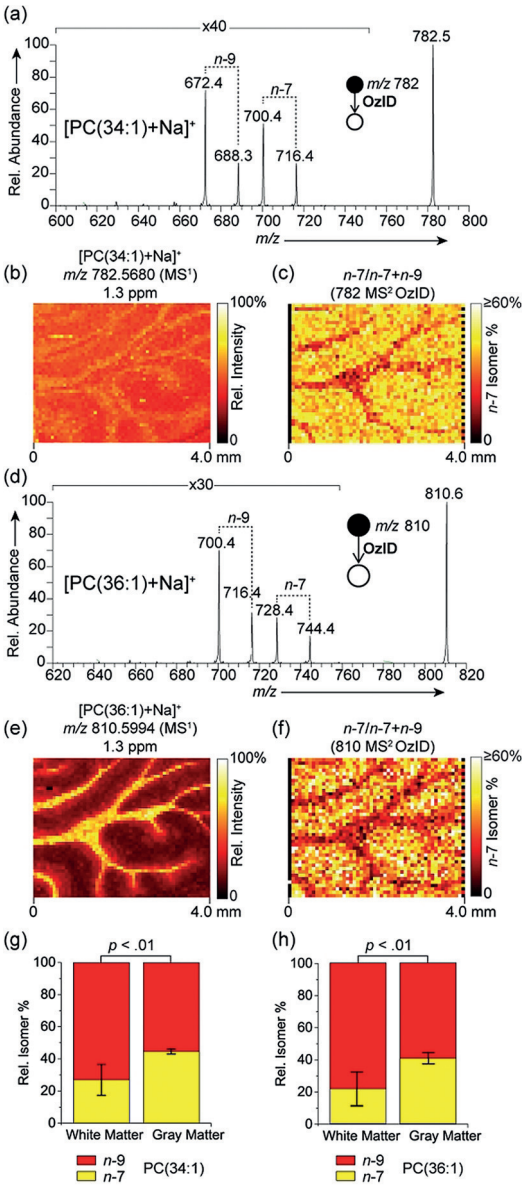

Figure 1. a) MALDI-OzID spectrum of $[PC(34:1)+Na]^+$ ions revealing the presence of $n-9$ and $n-7$ db isomers. b) The corresponding full-scan FTMS image of the $[PC(34:1)+Na]^+$ ion (m/z 782.5680) and c) fractional distribution image of $n-7$ and $n-9$ isomers ($(n-7)/(n-7+n-9)$) showing an enrichment of the $n-7$ isomer in the gray matter. d–f) Analogous spectra and images obtained for $[PC(36:1)+Na]^+$, again revealing an enrichment of the $n-7$ isomer in the gray matter. OzID and full-scan-FTMS data were acquired from consecutive tissue sections. Graphs show the $n-7$ and $n-9$ relative isomer percentages for g) PC(34:1) and h) PC(36:1) within the white and gray matter. Error bars represent coefficient of variation from each region ($n=5$ each for white and gray matter regions).

PC34:1($n-9$) isomer was observed in the white matter. These data reveal a differential and cell type-specific spatial distribution of lipid db-isomers in biological tissues with a relative circa 2-fold increase of PC34:1($n-7$) relative to isomeric PC34:1($n-9$) in the gray matter compared to the white matter (Figure 1 g). Importantly, given the near-identical chemical nature of these isomeric species, and thus

equivalent ionization efficiencies, the ratio images are unaffected by possible differences in desorption/ionization efficiencies or changes in concentration within different tissue regions. We note that these data reflect relative changes in product-ion abundance rather than absolute isomer concentrations, however, changes in FDI are a clear reflection of changing isomer populations across the tissue. An analogous assessment of PC(36:1) db-isomers was also performed (Figure 1 d–f). The full-scan MSI distribution revealed the summed image of all contributing isomers for the $[PC(36:1)+Na]^+$ ions and exhibited strong enrichment throughout the white matter. OzID analysis at each pixel revealed two distinct isomer populations and distributions corresponding to $n-9$ (m/z 700.4 and 716.4) and $n-7$ (m/z 728.4 and 744.4) isomers with their corresponding FDI revealing a significant relative enrichment of the $n-7$ isomer in the gray matter and the $n-9$ isomer in the white matter (Figure 1 f,h). These results provide the first demonstration of db-isomer resolution in MSI and suggest that individual lipid structural isomers play distinct roles in local cellular organization and metabolic processes. It is likely that our MSI results reflect the underlying local activity of certain desaturase and elongase enzymes that are involved in de novo lipid synthesis.[5] We also investigated db-isomers for polyunsaturated PC lipids (PC(36:2), PC(36:4) and PC(38:6)) but found significantly less isomeric diversity (Figure S2, Supporting Information).

Using sequential CID/OzID processes isomeric *sn*-positional variants could also be resolved and visualized throughout the rat brain. In the case of $[PC(34:1)+Na]^+$ (Figure 2 a), product ions confirmed the presence of PC(16:0/18:1) (m/z 379.3 and 395.3) and PC(18:1/16:0) (m/z 405.3 and 421.3) isomeric populations. Rationalization of these product ions is provided in Scheme S2 (Supporting Information).[10b] The full-scan MSI distribution of the precursor ion at m/z 782.5680 revealed a relatively homogenous distribution throughout the brain (Figure 2 b) and represents a composite distribution of isomers. However, the corresponding FDI (Figure 2 c) shows a subtle, yet significant (Figure 2 i) difference in the distribution of isomers. In the white matter PC(18:1/16:0) represents $31\pm3\%$ of the lipid isomer population made up of PC(16:0/18:1) and PC(18:1/16:0) and this increases to $43\pm2\%$ in gray matter. Importantly, for such monounsaturated *sn*-positional isomers relative CID/OzID product ion abundances have been demonstrated to reflect absolute isomer populations, and thus these results represent absolute molar fractions.[11c] Moreover, we observed an increase of LPC(18:1) relative to LPC(16:0) in the white matter (Figure S3, Supporting Information). Assuming PC(16:0_18:1) to be the largest source of these lyso lipids, these results suggest the possibility of increased phospholipase A1 activity in the white matter.

The underlying cell-specific selectivity of lipid isomer synthesis is further highlighted in the distributions of $[PC(36:1)+Na]^+$ *sn*-positional isomers (Figure 2 e–h). The resulting CID/OzID spectrum (Figure 2 e) revealed a complex fragmentation profile consistent with four unique isomeric structures, namely PC(18:0/18:1)/PC(18:1/18:0), and PC(16:0/20:1)/PC(20:1/16:0) isomer pairs with the full-scan Orbitrap MSI revealing the summed distributions to be

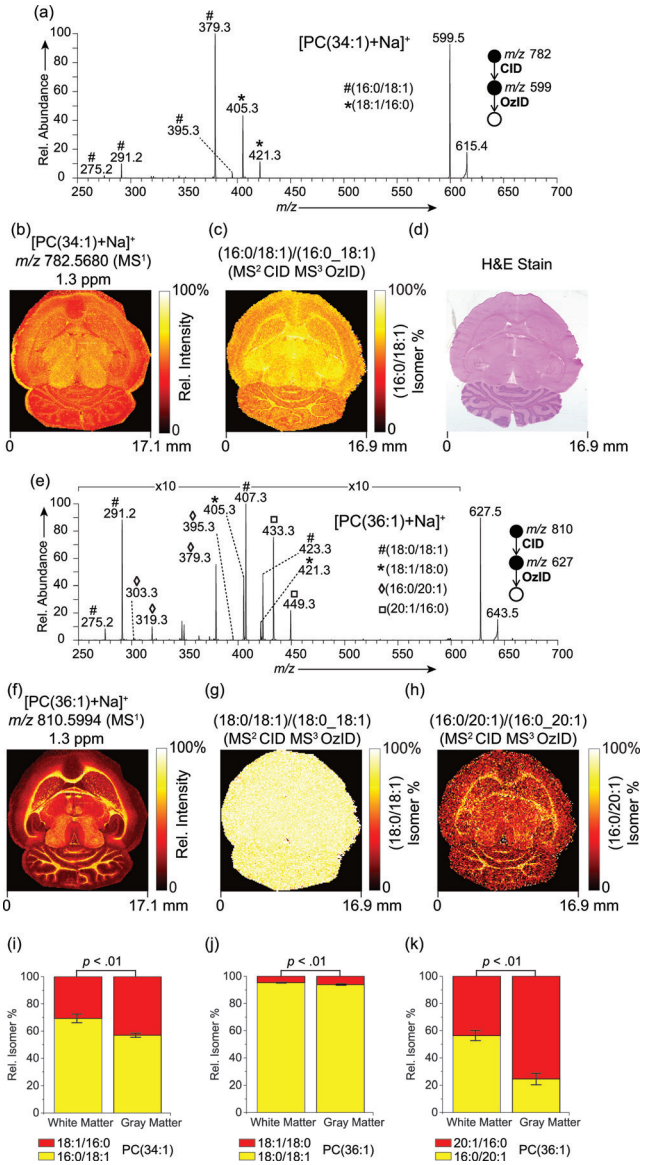

Figure 2. a) MALDI-CID/OzID spectrum of $[PC(34:1)+Na]^+$ ions revealing the presence of PC(16:0/18:1) and PC (18:1/16:0) structural isomers. b) The corresponding full-scan FTMS image of the $[PC(34:1)+Na]^+$ ion and c) fractional distribution image of PC(16:0/18:1) ions as a fraction of PC(16:0_18:1)-related ions. d) Post-acquisition stained tissue. e) MALDI-CID/OZID spectrum and f) full-scan FTMS image of $[PC(36:1)+Na]^+$ revealing the presence of four distinct *sn*-positional isomers (PC(18:0/18:1), PC(18:1/18:0), PC(16:0/20:1) and PC(20:1/16:0). The corresponding fractional distribution images of g) PC(18:0/18:1) as a fraction of PC(18:0_18:1); and h) PC(16:0/20:1) as a fraction of PC(16:0_20:1)-related ions. i–k) Graphs show relative isomer percentages for (i) the 16:0/18:1 and 18:1/16:1 isomers in PC(34:1); (j) the 18:0/18:1 and 18:1/18:0 isomers for PC(36:1); and (k) the 16:0/20:1 and 20:1/16:0 isomers for PC(36:1) within the white and gray matter. Error bars represent coefficient of variation ($n=5$ each for white and gray matter).

enriched in the white matter (Figure 2 f). Although product ions consistent with $[PC(18:0/18:1)+Na]^+$ (m/z 407.3 and 423.3) were circa 10-fold more abundant than those originating from $[PC(18:1/18:0)+Na]^+$ (m/z 405.3 and 421.3), the corresponding FDI (Figure 2 g) of these two isomers revealed

only a very slight (ca. 1%) alteration in isomer ratios between white and gray matter (Figure 2j). The additional CID/OzID product ions indicate a PC(16:0/20:1) and PC(20:1/16:0) isomeric pair (characteristic fragment ions at *m/z* 379.3/395.3 and 433.3/449.3, respectively). By contrast, the FDI of these two isomers exhibited a much more pronounced distinction between white and gray matter abundance (Figure 2h,k). $[PC(16:0/20:1)+Na]^+$ was significantly enriched in the white matter relative to isomeric $[PC(20:1/16:0)+Na]^+$, which was conversely enriched in the gray matter. Results from $[PC(32:1)+Na]^+$ (relative full-scan FTMS intensity of ca. 4%) are provided in Figure S4 (Supporting Information). These data highlight that isomer enrichments in tissues are highly specific and tightly regulated, with some isomeric pairs observed to change dramatically throughout different tissues (for example, white and gray matter, Figures 1 and 2c,h), while others do not change appreciably between brain regions (Figure 2g), even for lipids carrying some of the same acyl chains (see PC 16:0_18:1 and PC 18:0_18:1). CID/OzID analysis of a mouse brain containing a medulloblastoma tumor revealed altered and heterogeneous isomer populations in the tumor relative to the surrounding white and gray matter (Figure 3). The db-isomer distribution in this diseased tissue is provided in Supporting Information (Figure S5). This demonstrates the potential of targeted isomer-resolved imaging to study altered biochemical processes induced by disease.

Isomeric species differing in *sn*-position were also detected for a variety of polyunsaturated lipids, in particular PC(36:4) and PC(38:6), representing predominantly lipids containing 20:4 and 22:6 fatty acyl chains, respectively. It is often assumed in these cases that the polyunsaturated chain is

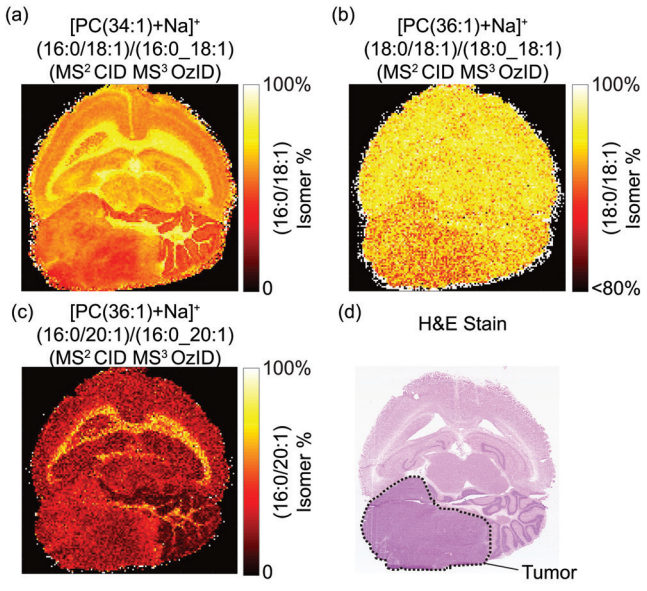

Figure 3. MALDI-CID/OzID fractional distribution images of a) PC(16:0/18:1) as a fraction of PC(16:0_18:1) structural isomers from $[PC(34:1)+Na]^+$ b) PC(18:0/18:1) as a fraction of PC(18:0_18:1) from $[PC(36:1)+Na]^+$ and c) PC(16:0/20:1) as a fraction of PC(18:0_18:1) from $[PC(36:1)+Na]^+$. These data were acquired from a mouse brain tissue section containing a medulloblastoma tumor. d) The post-acquisition H&E stained tissue, the tumor region is outlined in black.

specific to the *sn*-2 position.[14] CID/OzID analysis revealed both $[PC(16:0/20:4)+Na]^+$ and $[PC(20:4/16:0)+Na]^+$ contributing to PC(36:4), and both $[PC(16:0/22:6)+Na]^+$ and $[PC(22:6/16:0)+Na]^+$ contributing to PC(38:6) (Figure S6, Supporting Information). Furthermore, different spatial distributions were observed with lipids containing the polyunsaturated chain at the unexpected *sn*-1 position slightly enriched in the midbrain region. Most polyunsaturated phospholipids are synthesized through successive deacetylation–reacetylation steps involving phospholipase-driven removal of fatty acyls and reattachment of a polyunsaturated fatty acid onto the lyso lipid intermediate by lysophospholipid acyltransferase.[15] We hypothesize that the differential distributions of the above *sn*-positional isomers reflect the underlying relative activities of PLA1 and PLA2 enzymes that ultimately determine the available sites for acyl chain remodeling to occur. Such remodeling processes have previously been implicated in the enrichment of PC(18:1/16:0) in the tips of neuronal cells using isomer-specific fluorescent labels.[16]

We have observed for the first time differential distributions of both db- and *sn*-positional lipid isomers in biological tissues by exploiting gas-phase ion-molecule reactions that yield isomer-specific product ions. As with all MS/MS methods, our isomeric imaging approach is applied only to targeted precursor ions. However, the deployment of a multiplexed acquisition sequence enables multiple isomeric populations to be probed in a single experiment (Supporting Information). Moreover, while in this work ozonolysis reaction rates are limited by the gas requirements of the ion trap, alternative OzID implementations on instruments compatible with high concentrations of ozone (for example, certain q-ToF systems[17]) would offer faster acquisition speeds and increased sensitivity, and provides an exciting area of future research. Such approaches could even enable the assignment of db positions to individual *sn*-locations.[10b] Nonetheless, our data suggest that lipid isomer synthesis is highly conserved and dependent on local tissue type/environment (for example, white and gray matter in the brain). This high degree of structural specificity must reflect the localized activity of enzymes that synthesize and regulate lipid components (for example, fatty acids) and assemble complex lipids. Furthermore, these distributions reflect a biological need for distinct lipid isomer ratios that could confer distinct biophysical and biochemical properties.[18] The biological roles of individual lipid molecules and the reasons for the breadth of molecular complexity that they encompass are not well understood.[4a] In MSI, although many studies have reported altered lipid distributions throughout tissues, the biological origin of these altered lipid compositions is largely unknown, in part owing to the absence of isomer-level differentiation. In all MSI studies to date, lipid distributions represent an unresolved mixture of structural isomers that may not represent any one particular molecule or biological process. Our results provide a new avenue to overcome the limitations of current technology and deconvolute lipid MSI data down to the individually contributing lipid molecules that can begin to be rationalized through well-known enzymatic processes. Our innovative approach enables unraveling the biochemical

origins of lipid distributions observed throughout biology and studying the spatial distributions of structurally defined biomolecules with MSI, opening an avenue to unambiguous lipid imaging.

Experimental Section

All MSI experiments were performed using a Orbitrap Elite mass spectrometer (Thermo Fisher Scientific GmbH, Bremen, Germany) coupled to an intermediate pressure MALDI source (Spectroglyph LLC, Kennewick, WA, USA).[19] All brain sections were coated with norharmane matrix for MALDI-MSI analysis. Ozone-induced dissociation was conducted at each pixel by mixing high concentration ozone (ca. 14% (wt) in O_2) with the helium buffer gas entering the dual pressure ion trap. Further experimental details are provided in the Supporting Information.

Acknowledgements

This work was supported by the Dutch province of Limburg through the LINK program. S.R.E. and R.M.A.H. also acknowledge funding from Interreg V-A EMR and the Netherlands Ministry of Economic Affairs within the "EUR-LIPIDS" project (project number EMR23). Maastricht University gratefully acknowledges financial support from ITEA and RVO (project numbers ITEA151003/ITEA 14001). QUT authors acknowledge support from the Australian Research Council through the Discovery Program (DP150101715) and the CASS Foundation for travel support for D.L.M. The authors thank Tobey MacDonald at Emory University School of Medicine for providing mouse brain samples.

Conflict of interest

The authors declare no conflict of interest.

Keywords: biochemistry · brain · isomers · mass spectrometry imaging · phospholipids

How to cite: *Angew. Chem. Int. Ed.* **2018**, *57*, 10530–10534
Angew. Chem. **2018**, *130*, 10690–10694

[1] a) K. A. Zemski Berry, J. A. Hankin, R. M. Barkley, J. M. Spraggins, R. M. Caprioli, R. C. Murphy, *Chem. Rev.* **2011**, *111*, 6491; b) L. A. McDonnell, R. M. A. Heeren, *Mass Spectrom. Rev.* **2007**, *26*, 606; c) R. D. Addie, B. Balluff, J. V. M. G. Bovée, H. Morreau, L. A. McDonnell, *Anal. Chem.* **2015**, *87*, 6426; d) K. Schwamborn, R. M. Caprioli, *Nat. Rev. Cancer* **2010**, *10*, 639.

[2] a) J. M. Wiseman, D. R. Ifa, Q. Song, R. G. Cooks, *Angew. Chem. Int. Ed.* **2006**, *45*, 7188; *Angew. Chem.* **2006**, *118*, 7346; b) A. Römpp, S. Guenther, Y. Schober, O. Schulz, Z. Takats, W. Kummer, B. Spengler, *Angew. Chem. Int. Ed.* **2010**, *49*, 3834; *Angew. Chem.* **2010**, *122*, 3923.

[3] I. Lanekoff, K. Burnum-Johnson, M. Thomas, J. Short, J. P. Carson, J. Cha, S. K. Dey, P. Yang, M. C. Prieto Conaway, J. Laskin, *Anal. Chem.* **2013**, *85*, 9596.

[4] a) A. Shevchenko, K. Simons, *Nat. Rev. Mol. Cell Biol.* **2010**, *11*, 593; b) B. Brügger, *Annu. Rev. Biochem.* **2014**, *83*, 79.

[5] H. Guillou, D. Zadravec, P. G. P. Martin, A. Jacobsson, *Prog. Lipid Res.* **2010**, *49*, 186.

[6] K. F. Scott, M. Sajinovic, J. Hein, S. Nixdorf, P. Galettis, W. Liauw, P. de Souza, Q. Dong, G. G. Graham, P. J. Russell, *Biochimie* **2010**, *92*, 601.

[7] X. Ma, Y. Xia, *Angew. Chem. Int. Ed.* **2014**, *53*, 2592; *Angew. Chem.* **2014**, *126*, 2630.

[8] a) E. Ryan, C. Q. N. Nguyen, C. Shiea, G. E. Reid, *J. Am. Soc. Mass Spectrom.* **2017**, *28*, 1406; b) P. E. Williams, D. R. Klein, S. M. Greer, J. S. Brodbelt, *J. Am. Chem. Soc.* **2017**, *139*, 15681.

[9] a) T. Baba, J. L. Campbell, J. C. Y. Le Blanc, P. R. S. Baker, *Anal. Chem.* **2017**, *89*, 7307; b) J. L. Campbell, T. Baba, *Anal. Chem.* **2015**, *87*, 5837.

[10] a) M. C. Thomas, T. W. Mitchell, D. G. Harman, J. M. Deeley, J. R. Nealon, S. J. Blanksby, *Anal. Chem.* **2008**, *80*, 303; b) H. T. Pham, A. T. Maccarone, M. C. Thomas, J. L. Campbell, T. W. Mitchell, S. J. Blanksby, *Analyst* **2014**, *139*, 204.

[11] a) M. Groessl, S. Graf, R. Knochenmuss, *Analyst* **2015**, *140*, 6904; b) A. P. Bowman, R. R. Abzalimov, A. A. Shvartsburg, *J. Am. Soc. Mass Spectrom.* **2017**, *28*, 1552; c) A. T. Maccarone, J. Duldig, T. W. Mitchell, S. J. Blanksby, E. Duchoslav, J. L. Campbell, *J. Lipid Res.* **2014**, *55*, 1668; d) B. L. J. Poad, X. Zheng, T. W. Mitchell, R. D. Smith, E. S. Baker, S. J. Blanksby, *Anal. Chem.* **2018**, *90*, 1292.

[12] X. Ma, L. Chong, R. Tian, R. Shi, T. Y. Hu, Z. Ouyang, Y. Xia, *Proc. Natl. Acad. Sci. USA* **2016**, *113*, 2573.

[13] R. L. Kozlowski, T. W. Mitchell, S. J. Blanksby, *Sci. Rep.* **2015**, *5*, 9243.

[14] W. Stern, M. E. Pullman, *J. Biol. Chem.* **1978**, *253*, 8047.

[15] a) H. Shindou, D. Hishikawa, T. Harayama, K. Yuki, T. Shimizu, *J. Lipid Res.* **2009**, *50*, S46; b) H. Shindou, T. Shimizu, *J. Biol. Chem.* **2009**, *284*, 1.

[16] H. Kuge, K. Akahori, K.-i. Yagyu, K. Honke, *J. Biol. Chem.* **2014**, *289*, 26783.

[17] a) N. Vu, J. Brown, K. Giles, Q. Zhang, *Rapid Commun. Mass Spectrom.* **2017**, *31*, 1415; b) B. L. J. Poad, M. R. Green, J. M. Kirk, N. Tomczyk, T. W. Mitchell, S. J. Blanksby, *Anal. Chem.* **2017**, *89*, 4223.

[18] a) H. Martinez-Seara, T. Róg, M. Karttunen, I. Vattulainen, R. Reigada, *J. Phys. Chem. B* **2009**, *113*, 8347; b) M. F. Renne, A. I. P. M. de Kroon, *FEBS Lett.* **2017**, *591*, 1330; c) H. Martinez-Seara, T. Róg, M. Pasenkiewicz-Gierula, I. Vattulainen, M. Karttunen, R. Reigada, *Biophys. J.* **2008**, *95*, 3295.

[19] M. E. Belov, S. R. Ellis, M. Dilillo, M. R. L. Paine, W. F. Danielson, G. A. Anderson, E. L. de Graaf, G. B. Eijkel, R. M. A. Heeren, L. A. McDonnell, *Anal. Chem.* **2017**, *89*, 7493.

Manuscript received: March 12, 2018
Revised manuscript received: April 23, 2018
Accepted manuscript online: May 22, 2018
Version of record online: June 19, 2018

